

In-flight performances of the PAMELA satellite experiment

P. Papini^{d,*}, O. Adriani^d, M. Ambriola^j, G.C. Barbarino^g, A. Basili^a, G.A. Bazilevskaja^l, M. Boezio^e, E.A. Bogomolov^k, L. Bonechi^d, M. Bongi^d, L. Bongiornoⁱ, V. Bonvicini^e, A. Bruno^j, F. Cafagna^j, D. Campana^g, P. Carlson^f, M. Casolino^a, G. Castellini^c, J. Conrad^f, C. De Marzo^{j,1}, M.P. De Pascale^a, G. De Rosa^g, V. Di Felice^a, D. Fedele^d, A.M. Galper^b, P. Hofverberg^f, S.V. Koldashov^b, S.Yu. Krutkov^k, A.N. Kvashnin^l, J. Lund^f, J. Lundquist^e, O. Maksumov^l, V. Malvezzi^a, L. Marcelli^a, W. Menn^h, V.V. Mikhailov^b, M. Minori^a, S. Misin^l, E. Mocchiutti^e, A. Morselli^a, N.N. Nikonov^k, S. Orsi^f, G. Osteria^g, M. Pearce^f, P. Picozza^a, M. Ricci^l, S.B. Ricciarini^d, M.F. Runtso^b, S. Russo^g, M. Simon^h, R. Sparvoli^a, P. Spillantini^d, Yu.I. Stozhkov^l, E. Taddei^d, A. Vacchi^e, E. Vannuccini^d, S.A. Voronov^b, Y.T. Yurkin^b, G. Zampa^e, N. Zampa^e, V.G. Zverev^b

^aINFN, Structure of Rome Tor Vergata and Physics Department of University of Rome Tor Vergata, Via della Ricerca Scientifica 1, I-00133 Rome, Italy

^bMoscow Engineering and Physics Institute, Kashirskoe Shosse 31, RU-11540 Moscow, Russia

^cIFAC, Via Madonna del Piano 10, I-50019 Sesto Fiorentino, Florence, Italy

^dINFN, Structure of Florence and Physics Department of University of Florence, Via Sansone 1, I-50019 Sesto Fiorentino, Florence, Italy

^eINFN, Structure of Trieste and Physics Department of University of Trieste, Via A. Valerio 2, I-34127 Trieste, Italy

^fKTH, Department of Physics, Albanova University Centre, SE-10691 Stockholm, Sweden

^gINFN, Structure of Naples and Physics Department of University of Naples Federico II, Via Cintia, I-80126 Naples, Italy

^hUniversitat Siegen, D-57068 Siegen, Germany

ⁱINFN, Laboratori Nazionali di Frascati, Via Enrico Fermi 40, I-00044 Frascati, Italy

^jINFN, Structure of Bari and Physics Department of University of Bari, Via Amendola 173, I-70126 Bari, Italy

^kIoffe Physical Technical Institute, Polytekhnicheskaya 26, RU-194021 St. Petersburg, Russia

^lLebedev Physical Institute, Leninsky Prospekt 53, RU-119991 Moscow, Russia

Available online 18 January 2008

Abstract

PAMELA is a satellite-borne experiment designed to study with great accuracy charged particles in the cosmic radiation with a particular focus on antiparticles. The experiment, housed on board the Russian Resurs-DK1 satellite, was launched on June 15, 2006 in a 350 × 600 km orbit with an inclination of 70°. The apparatus comprises a time-of-flight system, a silicon-microstrip magnetic spectrometer, a silicon–tungsten electromagnetic calorimeter, an anticoincidence system, a shower tail catcher scintillator and a neutron detector. The combination of these devices allows charged particle identification over a wide energy range. In this work, the detector design is reviewed and the in-orbit performances in the first months after the launch are presented.

© 2008 Elsevier B.V. All rights reserved.

1. Introduction

The PAMELA (a Payload for Antimatter Matter Exploration and Light-nuclei Astrophysics) experiment is

installed inside a pressurized container attached to the Russian Resurs DK1 earth-observation satellite that has been launched into space by a Soyuz-U rocket on June 15, 2006 from the Baikonur cosmodrome in Kazakhstan. The satellite orbit is elliptical and semi-polar, with an altitude varying between 350 and 600 km, at an inclination of 70°. The mission is foreseen to last for at least three years.

*Corresponding author.

E-mail address: papini@fi.infn.it (P. Papini).

¹Deceased.

PAMELA has been designed to study charged particles in the cosmic radiation with a particular focus on anti-particles (antiprotons and positrons). The primary scientific goal is the study of the antimatter component of the cosmic radiation. Almost all data available so far have been obtained by balloon-borne experiments (see Ref. [1] for a compilation of data). PAMELA has been designed to perform very precise measurements with high statistics ($10^4 \bar{p}$ and $10^5 e^+$) and over a wider energy range (\bar{p} between 80 MeV and 190 GeV, e^+ between 50 MeV and 270 GeV). The precise determination of the antiproton and positron energy spectra will provide important information concerning cosmic-ray propagation and solar modulation.

Antiparticles could also be produced from the annihilation of dark matter particles (e.g. non-hadronic particles outside the Standard Model), which could lead to distortions of the measured spectra from pure secondary production. Unambiguous interpretation of exotic matter signature requires a clear understanding of the secondary spectra and their sources. Besides antiparticle measurements, PAMELA will perform precise measurement of the spectra and abundances of light nuclei and their isotopes; this will allow to test cosmic-ray propagation models and will help in reducing the uncertainties on the expected secondary-antimatter background.

Another prominent goal of PAMELA is to measure the $\overline{\text{He}}/\text{He}$ ratio with a sensitivity of the order of 3×10^{-8} . The contribution to the $\overline{\text{He}}$ flux from cosmic-ray interactions is expected to be completely negligible. Therefore an observation of $\overline{\text{He}}$ would represent an unequivocal signature of antimatter structures in the Universe.

The quasi-polar orbit and low geomagnetic cut-off experienced by the PAMELA apparatus, combined with its intrinsic ability to measure low momenta, allows phenomena connected with solar and earth physics to be investigated.

The ability to measure the combined electron and positron energy spectrum up to 2 TeV will allow the contribution of local sources to the cosmic radiation to be investigated.

The article is organized as follows. Section 2 provides an overview of the experiment, which includes a brief description of the apparatus and some details of the acquisition and trigger systems relevant to discuss the in-flight operations. In-flight performances of the instruments are shown in Section 3, where the capability of the experiment to achieve the science goals presented above is discussed.

2. Overview of the PAMELA apparatus

In this section a brief description of the apparatus is given, as an introduction to the following section where in-flight performances are discussed.

2.1. The PAMELA detectors

A schematic overview of the PAMELA is shown in Fig. 1. In the following the technical characteristics of each

detector is briefly summarized and its task in performing particle identification is described. More technical details about the instrument and its preparation to the launch can be found in Ref. [1] and references therein.

The central part of the PAMELA apparatus is a magnetic spectrometer consisting of a permanent magnet and a silicon tracking-system. The tracking system is composed by six equidistant planes of double-sided microstrip silicon detectors (six $300 \mu\text{m}$ thick $5.3 \times 7.0 \text{ cm}^2$ wide sensors), each providing two independent impact coordinates. The dimensions of the permanent magnet define the geometrical factor of the PAMELA experiment to be $21.5 \text{ cm}^2 \text{ sr}$.

The magnetic spectrometer is used to determine the sign of the electric charge and the rigidity ($R = cp/Ze$) of particles. The measured quantity is the deflection of a particle, which is defined as the inverse of the rigidity. The resolution in the deflection measurement is related to the spatial resolution of the silicon sensors. For normally incident tracks, tests with particle beams show a spatial resolution of (3.0 ± 0.1) and $(11.5 \pm 0.6) \mu\text{m}$ on the junction and ohmic side, respectively. Tests with proton beams show that a maximum detectable rigidity (MDR, defined as a 100% uncertainty in the measured rigidity) of 1 TV can be achieved. In flight, the deflection measurement of the tracking system is cross-checked with the energy measurement of the calorimeter for high-energy electrons. Silicon sensors also measure ionization losses, allowing absolute particle charge to be determined for $Z < 6$.

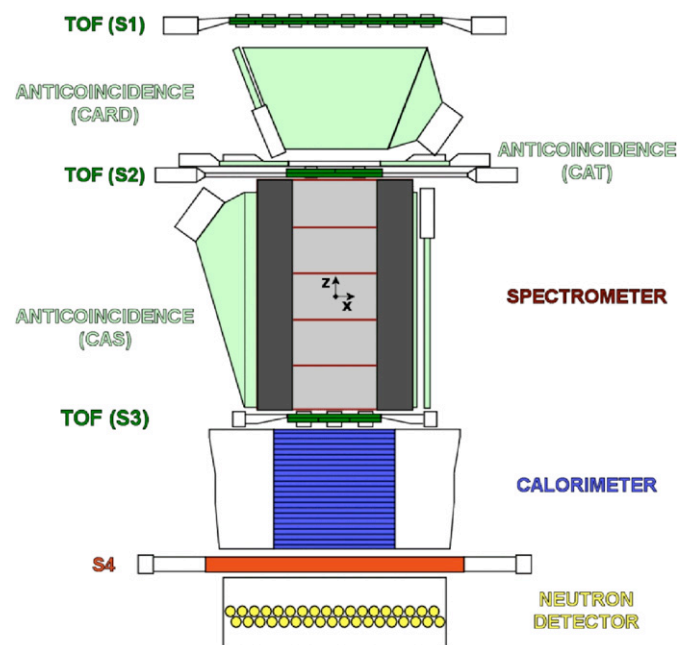


Fig. 1. Schematic overview of the PAMELA apparatus. The detector is approximately 1.3 m high, has a mass of 470 kg and an average power consumption of 355 W. The magnetic field lines inside the spectrometer cavity are oriented along the y direction. The average value of the magnetic field is $\langle B \rangle = 0.43 \text{ T}$.

The ToF system comprises six layers of fast plastic scintillators arranged in three double planes (S1, S2 and S3). Time-of-flight information for charged particles passing through planes S1 and S3 is combined with track-length information derived from the magnetic spectrometer to determine particle velocities. The measured time-of-flight resolution better than 300 ps allows $e^- (e^+)$ to be separated from $\bar{p} (p)$ up to 1 GeV/c. Albedo particles can also be rejected with a significance of 60 standard deviations. Ionization measurements in the scintillator layers allow the particle charge to be determined at least up to $Z = 8$.

A separate trigger board processes signals from the PMTs. Coincidental energy deposits in combinations of planes provide the main trigger for the experiment, as described in Section 3.2.

The sampling electromagnetic calorimeter comprises 44 single-sided silicon planes (nine 380 μm thick $8 \times 8 \text{ cm}^2$ wide sensors) interleaved with 22 plates of tungsten absorber. The total depth of the calorimeter is $16.3 X_0$ (0.6 nuclear interaction lengths). The main task of the calorimeter is to select e^+ and \bar{p} from backgrounds of particles with the same charge which are significantly more abundant (see Section 3.3). The longitudinal and transverse segmentation of the calorimeter, combined with the measurement of the particle energy loss in each silicon strip, allows a high identification (or rejection) power for electromagnetic showers against interacting and non-interacting hadrons.

The calorimeter is also used to reconstruct the energy of the electromagnetic showers. The constant term for the calorimeter energy resolution has been measured as 5.5% for electromagnetic showers generated by particles entering the calorimeter within the acceptance of the tracking system up to an energy of several hundred GeV. The calorimeter is also equipped with self-trigger capability. When a high energy-deposit is recorded, a fast signal is generated and processed by the trigger board, which can enable the event acquisition. This feature allows to detect particles which enter the calorimeter outside the tracker acceptance. With this wider instrument acceptance, the $e^- + e^+$ spectrum measurement can be extended up to $\sim 2 \text{ TeV}$.

The PAMELA experiment contains two anticoincidence (AC) systems: the primary AC system consists of four plastic scintillators (CAS) surrounding the sides of the magnet and one covering the top (CAT). A secondary AC system consists of four plastic scintillators (CARD) that surrounds the volume between the first two ToF planes. The aim of the AC systems is to identify false triggers, generated by secondary particles produced in the apparatus.

The shower tail catcher scintillator (S4) is a single scintillator plane placed below the calorimeter. The neutron detector is located below the S4 scintillator and consists of proportional counters filled with ^3He and surrounded by a polyethylene moderator. S4 and the

neutron detector complement the electron-proton discrimination capabilities of the calorimeter. The evaporated neutron yield in a hadronic shower is 10–20 times larger than expected from an electromagnetic shower. Joint analysis of the calorimeter and neutron detector information are expected to allow primary electron energies to be determined up to several TeV.

2.2. Data acquisition

PAMELA data acquisition system is based on the PSCU (PAMELA Storage and Control Unit), which comprises: a processor based on a RadHard ERC-32 CPU; two redundant 2 GByte mass memory modules; interface boards to subsystems and to Resurs satellite.

The PSCU automatically handles the flow of PAMELA physics tasks and continuously checks for proper operation of the apparatus. In parallel to acquisition of scientific data, once per second, the PSCU checks the information on voltages and alarms. In case of abnormal conditions the PSCU can perform a hardware reset of the whole system or, if insufficient to solve the problem (e.g. in case of electronics latch-up), powers down and then up PAMELA. The PSCU also checks the temperature environment by reading dedicated temperature sensors distributed in various locations around the instrument. If the readings exceed predefined values the PSCU powers down PAMELA until acceptable working conditions are reached. The PSCU also handles communication with the Resurs-satellite CPU and VRL (Very high-speed Radio Link) system.

The system can be remotely controlled through macrocommands and telecommands (hardware lines to handle power modules). Macrocommands are commands to the PSCU and can be sent either at request from ground or automatically by the Resurs CPU. Among other actions (data download operation, calibration, etc.), macrocommands allows to configure the system by setting proper parameters. In order to have an extremely flexible system, designed to be easily adapted to space (unknown) conditions, hundreds of modifiable parameters have been implemented in the PSCU software.

3. In-flight operations and performances

On June 21, 2006 PAMELA has been switched on for the first time. After a brief period of commissioning, during which several trigger and hardware configurations have been tested, PAMELA has been in a continuous data taking mode since July 11. Until March 2007, the total acquisition time has been ~ 213 days, for a total of ~ 460 millions of collected events and 3.7 TByte of stored raw data.

During this time some error conditions occurred, mainly attributable to latch-up events in the detector electronics. Every time the PSCU was able to recover the system functionality and continue the acquisition. The thermal

profile of the instrument resulted very stable and no power-off due to over temperature occurred. As an example, Fig. 2 shows the temperature profile measured at one of the

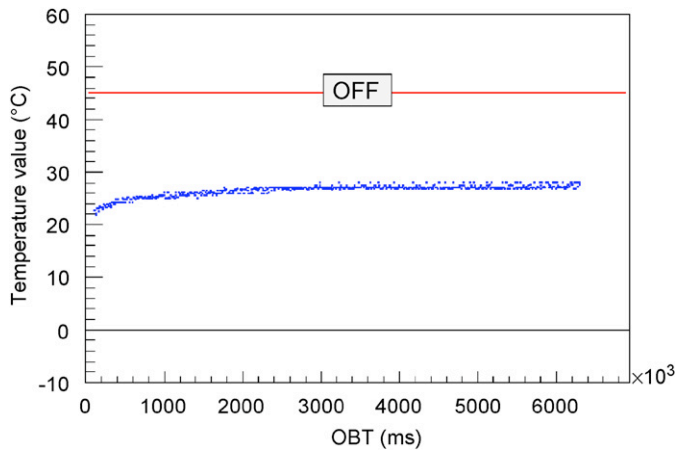


Fig. 2. Temperature profile of one of the interface power modules during the first PAMELA power on, as a function of the on-board time. Also indicated is the maximum allowed temperature value. If the temperature exceeds this limit the system is temporarily powered down.

interface power modules, during the first PAMELA power on. The system was on for about 2 h. The temperature increased slowly at power on and became stable at a value of $\sim 26^\circ$ after about 30 min.

3.1. The orbital environment

PAMELA instrument is equipped with several counters that measure particle rates independently from the trigger.

Fig. 3 (top) shows the particle rates measured by the three ToF planes, S1 (higher rate), S2 and S3 (lower rate), as a function of the on-board time. The duration of an orbit is ~ 95 min. The maxima at ~ 150 S1 counts (over 60 ms) correspond to passages over the polar regions (NP and SP), while the minima correspond to passages over the equator (EQ). The prominent peaks close to the equator indicate the passage inside the South Atlantic Anomaly (SAA). Here the rate on S1 is so high to saturate the counter. Also visible in the S1 counts are structures due to passages inside the outer radiation belt, which occurs close to the South Pole, where, at the time when these data were collected, the satellite altitude was close to its maximum value.

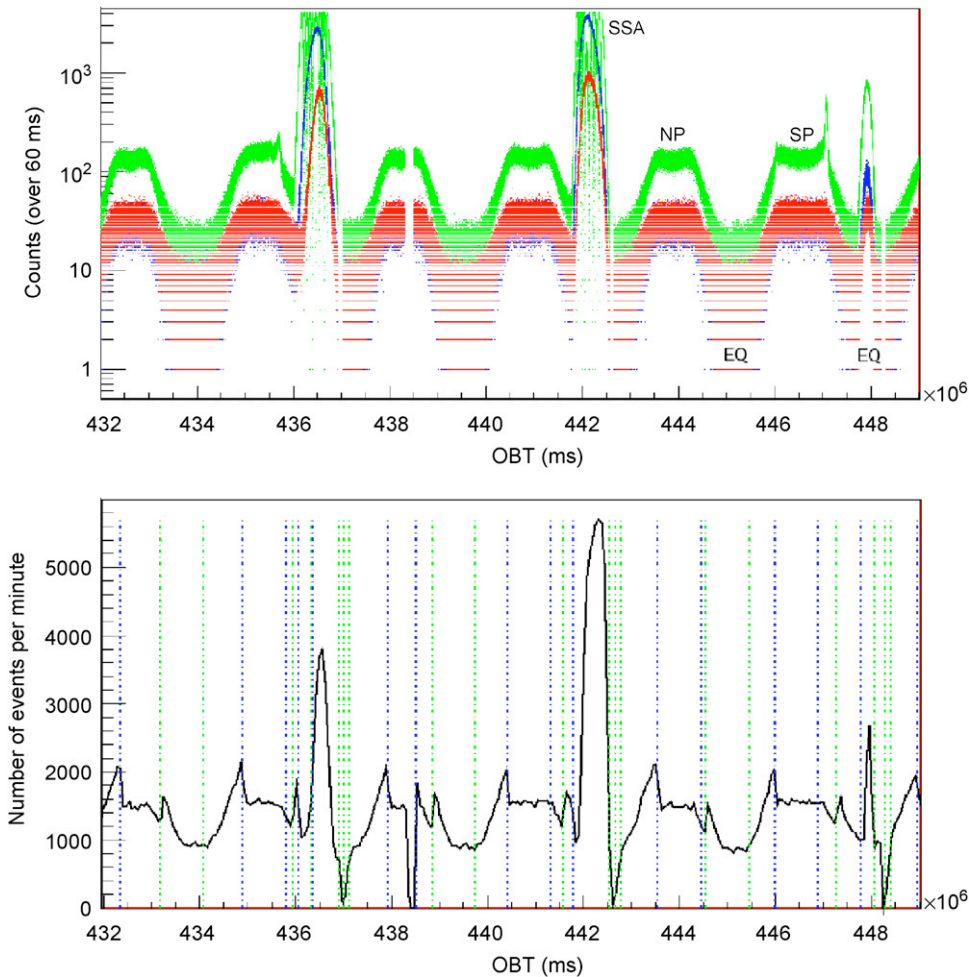


Fig. 3. *Top*: Particle rates measured by S1, S2 and S3 as a function of the on-board time, for three consecutive orbits. *Bottom*: Trigger rate (expressed in events per minute) as a function of the on-board time, over the same orbits shown above. Vertical dashed lines indicate start-time of different runs. Rates are strongly dependent on the orbital position (see the text for explanations).

The gaps in the data at the equator, soon after the SAA, indicate the positions where the apparatus is calibrated. By default, the calibration is performed at the point of lowest particle rate, which occurs when the satellite crosses the equator from the southern to the northern hemisphere. This position is notified at every orbit by the Resurs CPU by issuing a dedicated macrocommand.

The plot in Fig. 3 (top) is obtained from the data transmitted in a typical download session (transfer of the 2 GByte PAMELA mass memory content into the Resurs mass memory), which covers a time interval of about 5 h. The wider gap during the second passage through the northern polar region indicates where previous download was performed, about 3 h before. On average, time intervals covered by single downloads overlap, giving redundancy in data transmission.

Other rate meters are implemented in the PAMELA apparatus (rate of particles hitting ACs, rate of background neutrons, etc.), which provide useful information about the space radiation environment.

3.2. Trigger rate

The data acquisition is segmented in runs, defined as continuous period of data taking with constant detector and trigger configurations. The duration of a run is determined by the PSCU according to the orbital position. Two acquisition modes are implemented, for high- and low-radiation environments. The run configuration, in both acquisition modes, and the criterion to switch between low- and high-radiation environments can be varied from ground. A total of 29 trigger configurations have been implemented, including various ToF-layer combinations, with or without calorimeter self-trigger and S4 trigger.

The configuration that was found to maximize the collected number of good cosmic-ray events is the following (the subscripts 1 and 2 refer to the upper and lower layers in each ToF plane).

Low-radiation: [(S₁₁ or S₁₂) and (S₂₁ or S₂₂) and (S₃₁ or S₃₂)] or calorimeter.

High-radiation: [(S₂₁ and S₂₂) and (S₃₁ and S₃₂)] or calorimeter.

In the trigger configuration for low-radiation environment the upper and lower layers of each ToF plane are combined with an *or* condition, in order to allow efficiency studies. The highest rate is recorded inside the SSA, where most of the particles have very low energy. Since only S1 is affected by SSA radiation, this plane has been excluded from the trigger condition for high-radiation environment; in addition, all ToF layers are combined with an *and* condition in order to further reduce the trigger rate. Switch between the two acquisition modes is performed when the counting rate of S1 exceeds a given threshold.

The bottom plot in Fig. 3 shows the trigger rate of PAMELA. Vertical lines indicate start-time of different

runs. The discontinuities in the trigger rate are due to switching between the two acquisition modes for high- and low-radiation environment. Outside the radiation belt, the average rate is ~ 25 Hz, while inside the SSA the rate saturates.

3.3. Particle identification capabilities

In this section some preliminary results concerning in-flight performances of the PAMELA instrument are presented. Calibration of the instrument is still under progress and significant improvements are expected in the near future. Nevertheless, results show that PAMELA is working in nominal conditions.

A basic step in particle identification is the charge selection. This is performed mainly by means of the energy-deposit measurements in the tracker and ToF layers. Fig. 4 (top) shows the average dE/dx measured by the tracker as a function of the rigidity, obtained for a sample of positively charged particles from flight data. The good separation among different charge families is evident from the plot, even from this preliminary analysis. Furthermore, at low rigidities also H and He isotopes can be distinguished. Above Be tracker detectors saturate and, consequently, charge-identification performances are significantly reduced. Both tracking system and ToF are designed to have best performances for light particles. Nevertheless, charge identification of heavier nuclei is possible by means of the calorimeter, because its silicon detectors have a much wider dynamical range. Fig. 4 (bottom) shows the dE/dx measured by the first silicon plane of the calorimeter (which is placed above the first tungsten plane), for a sample of nuclei roughly selected with the tracker by rejecting H and He. Nuclei from Li to O can be clearly distinguished.

The main task of PAMELA is to identify antimatter components against the most abundant cosmic-ray components. The relative abundance of collected matter and antimatter particles can be roughly inferred from Fig. 5, where the ratio between the signal collected by the calorimeter and the rigidity measured by the spectrometer is shown, for a small sample of flight data. On the negative side, the most prominent feature is an horizontal band that represent the electron component. In this case almost all the particle energy is deposited inside the calorimeter, resulting in a constant energy/rigidity ratio. Antiprotons, either interacting or non-interacting, deposit on average a small fraction of their energy inside the calorimeter and lay below the electron band. On the positive side the distribution is dominated by protons.

Main sources of background in the antimatter samples come from spillover (p in the \bar{p} sample and e^- in the e^+ sample) and from like-charged particles (e^- in the \bar{p} sample and p in the e^+ sample).

Spillover background comes from the wrong determination of the charge sign due to measured deflection uncertainty; its extent is related to the spectrometer

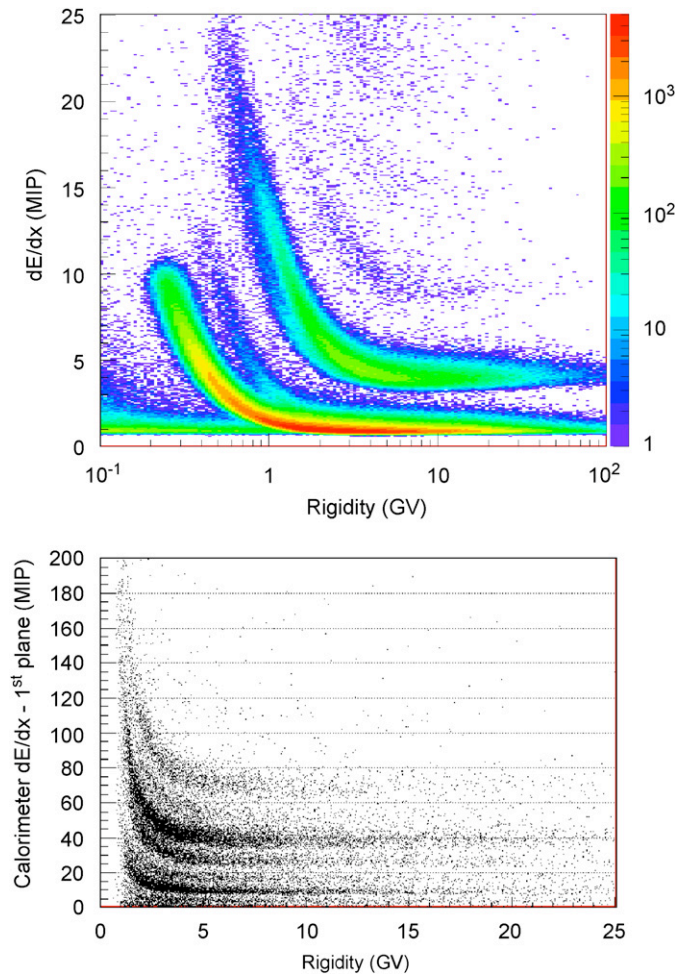


Fig. 4. Top: dE/dx measured by the tracking system as a function of the measured rigidity. Bottom: dE/dx measured by the first silicon plane of the calorimeter as a function of the measured rigidity (most of H and He nuclei have been removed by applying a cut on the dE/dx measured by the tracker).

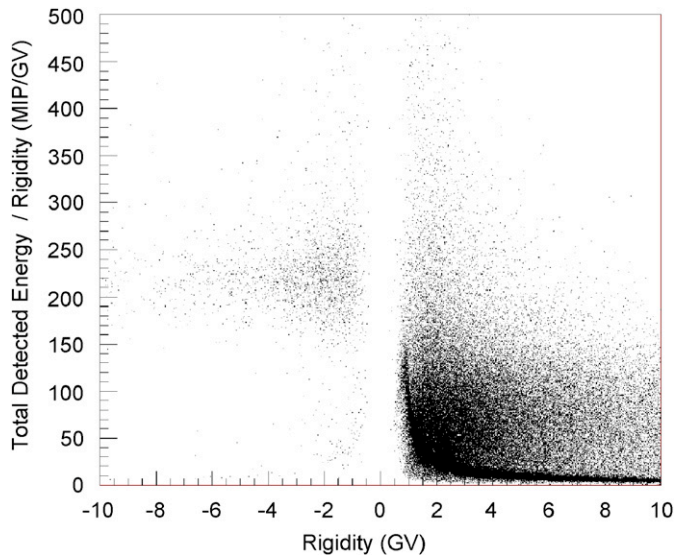


Fig. 5. Ratio between the signal collected by the calorimeter and the rigidity measured by the spectrometer. Negative rigidities indicate negatively charge particles.

performances and its effect is to set a limit to the maximum rigidity up to which the measurement can be extended.

The like-charged particle background is related to the capability of the instrument to perform electron-hadron separation. Therefore, the most unfavorable regions are at low energy for \bar{p} and at high energy for e^+ , where the natural relative abundance of background particles (e^-/\bar{p} and p/e^+) exceeds 10^3 . This means that the PAMELA system must separate electrons from hadrons at a level of 10^5 – 10^6 . Much of this separation must be provided by the calorimeter, i.e. electrons must be selected with an acceptable efficiency and with as small a hadron contamination as possible. At low energy, below ~ 1 GV, additional information for particle identification is provided by the ToF system and the tracker dE/dx . At high energy the hadron rejection factor can be improved by using neutron detector information.

Fig. 6 shows a ~ 11.6 GV negatively charged interacting hadron, most likely an antiproton and Fig. 7 shows a ~ 32.3 GV positively charged electromagnetic particle, most likely a positron. Electron events have the same characteristics of positron events, but for the sign of trajectory curvature. The typical features of hadronic and electromagnetic showers can be easily distinguished by comparing the particle patterns inside the calorimeter. The calorimeter has been proven to provide (from test beam data) a proton rejection factor of about 10^5 in selecting positrons and electrons and (from simulations) an electron rejection factor of about 10^5 in antiproton measurements, while keeping in both cases about 90% efficiency [1]. By comparing Figs. 6 and 7, it is also evident the different signature in the neutron detector. The additional

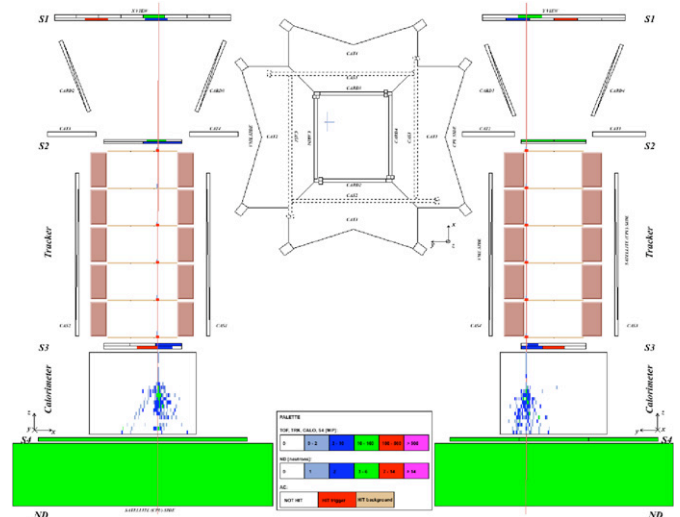


Fig. 6. The event display a ~ 11.6 GV interacting antiproton. The bending (x) and non-bending (y) views are shown on the left and on the right, respectively (plane 19 of the calorimeter x -view was malfunctioning). A plan view of PAMELA is shown in the center. The signal as detected by PAMELA detectors are shown along with the particle trajectory (solid line) reconstructed by the fitting procedure of the tracking system.

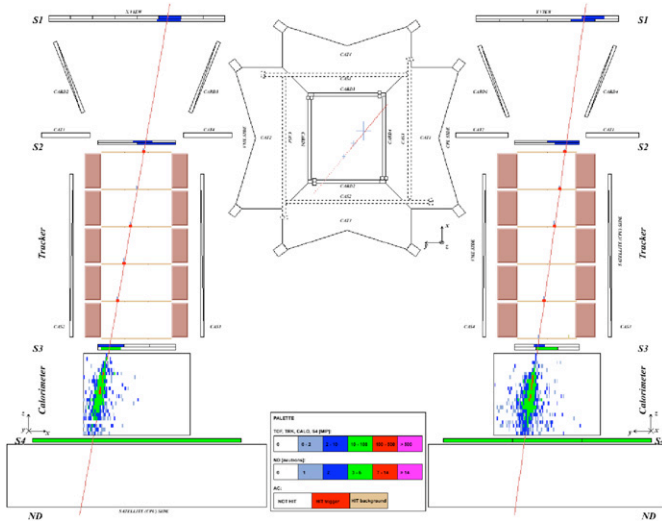


Fig. 7. The event display a ~ 32.3 GV positron. The bending (x) and non-bending (y) views are shown on the left and on the right, respectively (plane 19 of the calorimeter x -view was malfunctioning). A plan view of PAMELA is shown in the center. The signal as detected by PAMELA detectors are shown along with the particle trajectory (solid line) reconstructed by the fitting procedure of the tracking system.

hadron-rejection power provided by the neutron detector increases for increasing energy.

The calorimeter potentialities in performing electron/hadron separation are illustrated in Fig. 8. Data from several days of acquisition were used. On the top figures, the ratio between the energy released along the particle trajectory inside the calorimeter and the total deposited energy is shown, for negative (first plot) and positive (second plot) particles. The energy deposit of non-interacting particles is localized along the trajectory, resulting in a peak at 1; electromagnetic particles deposit an almost constant fraction of the energy along the trajectory (about half of the energy, with the selection condition adopted in Fig. 8); interacting hadrons are characterized by large fluctuations in shower development, resulting in an almost flat distribution spanning from 0 to 1. In the first plot the electron and non-interacting antiproton contributions are evident; in the second plot only protons can be distinguished, the small positron component being overwhelmed by interacting protons. On the bottom side of Fig. 8 the same histograms as described above are shown, after the application of a preliminary set of cuts aimed to select electromagnetic showers. The calorimeter provides several discrimination criteria, based on both energy release and shower topology. By using this information it is possible to extract the positron component, as it is shown in the fourth plot of Fig. 8.

4. Conclusions

The PAMELA satellite experiment aims to perform precise measurement of cosmic-ray spectra over a wide

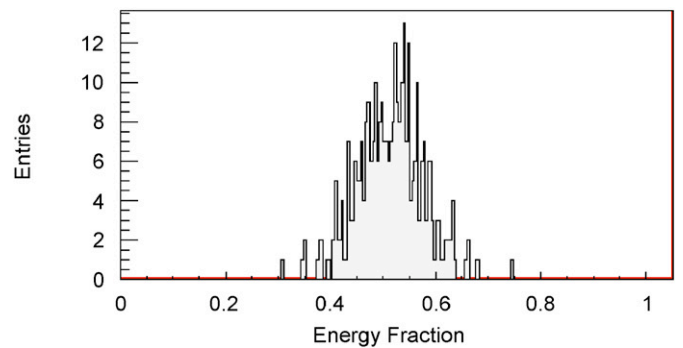
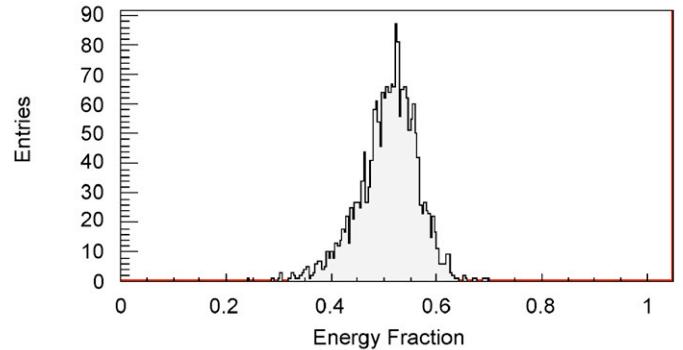
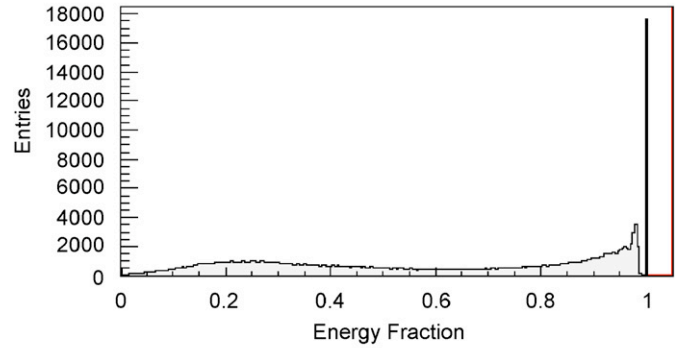
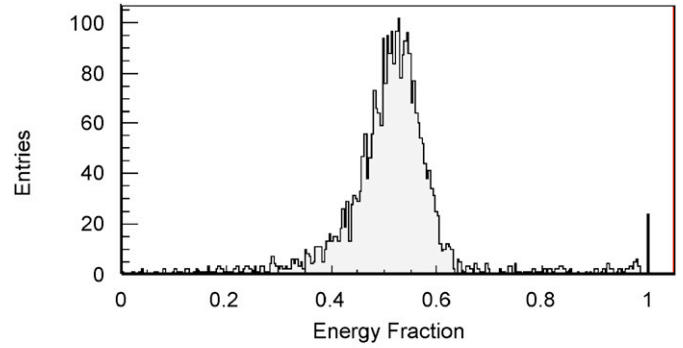


Fig. 8. *Top figures:* Fraction of the total energy deposited along the particle trajectory inside the calorimeter, for negative (first plot) and positive (second plot) particle. *Bottom figures:* Same as top ones after the application of cuts aimed to select electromagnetic showers. After the cuts the small positron component emerges from the proton background (fourth plot). See the text for more explanations.

energy range, with special focus on antimatter components. In order to achieve these goals, for the first time the combination of a microstrip-silicon magnetic-spectrometer

and a silicon–tungsten imaging calorimeter has been sent in space. The satellite has been successfully launched on the June 15, 2006. Detectors did not suffer any damage due to the launch and the experiment is almost continuously taking data since then. A preliminary analysis of flight data indicates that individual detectors are performing nomin-

ally. Results of great scientific relevance are expected from the PAMELA experiment.

Reference

- [1] P. Picozza, et al., *Astro. Phys.* 27 (2007) 296.